German J Pharm Biomaterials 2023; 2(4): 19-30
https://doi.org/10.5530/gjpb.2023.4.12

GJPB

Research Article

Venonia amygdalina leaf extract - mediated redox synthesis of silver nanoparticles: Characterization and antimicrobial activity

Romanus C. Omeh[1]*, Ibeabuchi Jude Ali[2], Cyril Ckekwube Adonu[3]

[1]Department of Pharmaceutics and Pharmaceutical Technology, Faculty of Pharmaceutical Sciences, Enugu State University of Science and Technology, Enugu State, South East Nigeria.
[2]Department of Pharmaceutical Chemistry, Faculty of Pharmaceutical Sciences, Enugu State University of Science and Technology, Enugu State, South East Nigeria.
[3]Department of Pharmaceutical Microbiology and Biotechnology, Faculty of Pharmaceutical Sciences, Enugu State University of Science and Technology, Enugu State, South East Nigeria.

*Correspondence: romanus.omeh@esut.edu.ng

Received: 16 June 2023; Revised: 15 August 2023; Accepted: 25 August 2023

Abstract

The synthetic process, type of precursor material, and the phytochemical materials involved in the biological synthesis of metal nanoparticles influence the properties of the resulting nanoparticles. The physicochemical attributes of synthesized nanoparticles, in turn, influence their applicability for various purposes, hence the need to standardize synthetic processes and characterize nanoparticle outputs for reproducibility and optimal utility. The objective of this study was to utilize bitter leaf (*Vernonia amygdalina*) extract in the synthesis of silver nanoparticles (AgNPs), characterize the nanoparticles, and then evaluate the same for antimicrobial activities. The *V. amygdalina* extract was produced by the soxhlet extraction process after the leaves were subjected to standard pre-extraction treatments using methanol as the extraction solvent. The solid extract was separated by rotary evaporation, and a predetermined quantity was mixed with 0.1 M silver nitrate solution under controlled concentration, temperature, and pressure. The resulting nanoparticles were characterized for morphological, optical, spectroscopic, and other physicochemical properties and then evaluated for antibacterial activities. The mean particle size, polydispersity index, and zeta potential of the nanoparticles were 74.231 ± 0.43 nm, 0. 645 ± 0.04, and 32.045 ± 0.054 mV, respectively. The Fourier transform infrared analysis suggested an association between the silver nanoparticles and the extract biomolecules, while x-ray diffraction showed particle crystallinity. The nanoparticles were effective against selected Gram-positive and Gram-negative bacteria. It was concluded that the procedure and materials used resulted in the synthesis of silver nanoparticles from the silver nitrate salt through a biogenic reduction process.

Keywords: Nanoparticle; biogenic process; biomolecules; Venonia amygdalina; bitterlea; fungicidal

Introduction

Nanomaterials may be described as substances consisting, in whole or parts, of particles having size distribution within the range of 1-100 nm and in which the ultra-fine sizes confer on the material some unique characteristics that were lacking or less prominent in their original larger-sized source materials. Upon attaining the nanosized structure, materials characteristically acquire many novel physicochemical characteristics that make them more useful and functional than their macro-sized counterparts. Basically, such materials exhibit markedly reduced weight-to-volume ratio accompanied by amplified surface area, enhanced optical and magnetic properties as well as exaggerated reactivity. Nanosized drugs are reported to exhibit higher solubility, greater membrane permeability, and enhanced bioavailability, making them ideal platforms for both local and systemic drug delivery. Such acquired properties of nanomaterials are also being utilized in novel ways in virtually all fields of

human endeavors, including agriculture, sports, intelligence systems, and security, as well as in the medical and pharmaceutical sciences and other specialties. The nature of their precursor materials equally significantly influences the applicability of some nanomaterials for specific purposes, the fabrication technology deployed, the processing environment, and often, the materials used in their synthesis. The functionalities of many nanomaterials are also affected by their physicochemical properties, such as shapes, powder morphology, particle size distribution, crystalline structures, surface charges, and other specific characteristics. Although many previous workers had synthesized AgNPs using mechanical, chemical, and biological processes [1-3], to the best of our knowledge, only Aisida et al. [4] utilized bitterleaf (*V amygdalina)* extract for such synthesis. Unlike the aqueous solvent used by these authors in a hot maceration technique, the current work utilized a less polar solvent, methanol, in a soxhlet process to harvest the extract. This was in consideration of the fact that some of the bioactive principles in the leaves may show preferential solubility in nonpolar solvents and a thermally-assisted extraction process. A successful synthesis of AgNPs through the current process will offer a comparison between distilled water and methanol-based extracts in terms of the physicochemical characteristics of AgNPs synthesized using the two extraction solvents in two different processes. The conflicting relative abundance of tannins in *Vernonia* amygdalina (V. amygdalina) leaf extract, as reported by different authors, will also be investigated.

Many technologies have been utilized for the preparation of nanoparticles. These processes are broadly classified as top-down and bottom-up techniques. While top-down methods involve the breakdown of materials from larger sizes to smaller sizes at the nanoscale level, bottom-up methods involve the aggregation or build-up of atomic or molecular-sized materials to nanoscale sizes. Top-down processes may be achieved by mechanical milling, thermal/laser ablation, chemical etching, and microwave and ultrasonic wave applications, among others [5]. Bottom-up methods, on the other hand, involve one or more of the following processes: spray drying, spray pyrolysis, flame spray pyrolysis, molten metal atomization, wet chemistry, biological synthesis, and incidental formation of nanoparticles [6].

Biological/biogenic synthesis of nanomaterials involves the use of biological or bioactive materials found in biological species like bacteria, fungus, algae, and plant extracts to mediate chemical reaction processes that result in the reduction of metallic salts to their pure metal or metal oxide nanoparticles [7]. This process has gained wide acceptance as a preferred alternative to the other traditional methods due to the many advantages it offers. The process is generally simple, devoid of the use of toxic chemicals, and does not require high energy inputs. It is also environmentally friendly, and the useful biological materials are widely available and cheap. Biological processes are also amenable to control, just as the end products can be manipulated or functionalized to suit specific application purposes [8, 9]. It has been established that phytochemical constituent of plant extracts like phytosterols, flavonoids, and saponins play the role of reducing and stabilizing agents during the chemical interaction between the extract and the metal salts [10].

V. amygdalina, which is generically known as a bitter leaf, is a perennial shrub belonging to the taxonomic family *Asteraceae* and the genus *Vernonia*. It grows in many tropical climates, particularly within the West African region [11]. It is called by many local names in different cultures, including Onugbu, Ewuro, Fatefata, and Eriwo, by various tribes in Nigeria [12]. In Ghana, it is popularly known as Awonwon [13], while the Togolese call it Aluma [14].

Previous research has reported the high content of phenolic compounds, saponins, alkaloids, and flavonoids in bitter leaf extracts [15,16]. This invariably makes the extract a good candidate for the biological synthesis of AgNPs. Similarly, the use of *V. amygdalina* extracts for traditional management of suspected cases of cancer, diabetes, neurological pains, malaria, high blood pressure, anemia, and other disease conditions has been separately reported by Akah et al. [17] and Ugwu et al. [18]. V amygdalina-based AgNPs may, therefore, produce a synergy between the therapeutic effects of the plant extract and the known therapeutic activities of AgNPs. The current work, therefore, not only synthesized and characterized AgNPs but also investigated the existence of possible synergistic

antimicrobial effects resulting from the conjugation of the nanoparticles and the biomolecules of the *V. amygdalina* extract by comparing the antimicrobial zones of inhibition caused by the raw extract, pure $AgNO_3$ and the synthesized AgNPs against reference antimicrobial drugs. Although a number of researchers have investigated the prospect of biological synthesis of AgNPs using plant extracts [19-21] the use of *V. amygdalina* extract for this purpose with the extensive characterization of the resulting nanoparticles has, to the best of our knowledge, been scarcely done. The current work may, therefore, be a good addition to the existing knowledge of the synthesis, characterization, and antimicrobial activity of AgNPs.

Materials And Methods

Materials

Mature fresh leaves of *V. amygdalina* were collected from the Demonstration Farms of the Department of Crop Science, University of Nigeria Nsukka, Enugu State, Nigeria, in July 2022. AgNO3 (anhydrous - 99.80 %), swab sticks, Muller Hinton broth, and Muller Hinton agar were products of Sigma Aldrich, Germany, while Staphylococcus aureus (Staph aureus), Escherichia coli (E coli), Exiguobacterium aquaticum (E aquaticum) and Candida albican (C albica) were gifts from Adonai Medical Diagnostic Laboratories, Nsukka, Enugu State, Nigeria, Reference samples of Ciprofloxacin and Amphotericin B were obtained from Juhel Pharmaceutical Industries, Nigeria. All other chemicals and reagents used in the study were obtained from a licensed chemical vendor, Jeochem (Nig) Ltd, Nsukka, Nigeria, and were used as supplied except otherwise specified.

Methods

Plant material collection preparation and extraction of constituents

The plant sample was identified by Mr. S. M. Ozioko (a Taxonomist) at the Bioresource Centre, Obechara Roundabout, Nsukka, Enugu State, Nigeria, who also gave a sample identity number, BRC/2022/15PR and archived a voucher specimen in the Centre's herbarium. Prior to use, the leaves were treated according to the method reported by Aisida et al. [4]. In brief, the leaves were washed thrice under running tap water, then rinsed with distilled water, and subsequently dried under shade for 14 days. The dry leaves were finally milled to coarse powder with a domestic electric grinder (LP/Bx/071). A total of 2000 gm of the powder was extracted in eight batch runs of 250 gm per batch using 400 ml of methanol for each batch on a soxhlet equipment (SE-6P, BIOEVOPEAK INC. USA). The crude extract was filtered through a No 1 Whatman filter paper, and the filtrate was concentrated on a rotary evaporator (Hei-Vap Core, Heidolph Instruments, GMB Germany). The gummy residue was freeze-dried to soft powder using a vacuum pressure-low temperature freeze drier (Decibel Digital Technology, India).

Phytochemical analysis of bitterleaf extract

Various standard methods reported for determining phytoconstituents of extracts were used in the current studies, and these included Molisch's test for carbohydrates and other specific qualitative tests for saponins, flavonoids, alkaloids, and tannins: terpenoids, steroids, and phenolic constituents [16]. The relative abundance of each component was indicated with plus signs, with one, two, and three plus signs indicating low, moderate, and high concentrations of constituents, respectively. The absence of a component was indicated with a minus sign.

Synthesis of AgNPs

Biogenic synthesis of metal nanoparticles generally involves reduction reactions between biological metabolites like polyphenolic compounds, polysaccharides, amino acids, alkaloids, and vitamins, among others, and metal salts or ions in which the metabolite acts as the reducing and stabilizing (capping) agents for the conversion of metal salts/ions to zero valence metal nanoparticles [22]. In the current work, 1 ml of *V amygdalina* leaf extract was added in a dropwise manner to a 100 ml volume of a 0.001 M solution of silver nitrate contained in a 250 ml capacity conical flask. The reaction was carried out under a controlled temperature of 80 ºC with the pH adjusted to 10 with 0.1 M NaOH solution and

under continuous shaking. The process was closely observed until a sudden change in the color of the mixture was observed. These reaction parameters have been reported to be optimum for greater yield and reproducible quality of the AgNPs [23]. The mixture was then centrifuged (Omega 4 Centrifuge) at 20,000 rpm for 25 min, which resulted in the sedimentation of some precipitates. The supernatant was decanted, leaving some soft pellets. The pellets were washed six times with double distilled water, followed by rinsing with 90% ethanol to improve the purity of the synthesized AgNP powder [4].

Characterization of AgNPs

UV spectral analysis of AgNPs

The UV spectral analysis of the sample was determined in triplicate using a UV spectrophotometer (JENWAY 7305, Germany). A 30 mg/ml solution of the synthesized AgNPs was scanned through 300 - 600 nm wavelengths. The values generated were used to construct the UV-visible light absorbance spectrum from which the wavelength of maximum absorbance (λ_{max}) was determined.

Spectroscopic, microscopic and antimicrobial activity analysis of AgNPs

The synthesized AgNPs were also subjected to relevant microscopic, spectroscopic, and antimicrobial analysis to elucidate their physicochemical, morphological, and antipathogen attributes. Sample preparations for the tests were done according to the method of Droepenu et al. [24] and Droepenu et al. [25], while equipment operation was according to manufacturers' guidelines.

The mean particle sizes (Z-Average), polydispersity index, and zeta potential of the samples were studied on a dilute suspension of the nanoparticles using the dynamic light scattering equipment (Zeta-Nano, Model ZEN3600, Malvern Paralytical, United Kingdom). The equipment was designed to measure the three parameters concurrently. A scanning electron microscope (SEM) (SU3500, Hitachi) and a Transmission electron microscope were used to study the surface morphology of the nanoparticles. In contrast, the X-ray diffraction studies for the structural elucidation of the AgNPs powder were conducted on a Shimadzu- 7000 madel Powder X-ray diffractometer equipped with Cu-Kα radiation capacity of λ = 1.5406 Å and set at a continuous scanning range (2θ) of 15 - 80 ºC at room temperature. The functional groups present in the AgNPs were investigated using a Fourier transform infrared (FTIR) spectrometer (Agilent Technologies USA). In brief, a thin smear of the sample dissolved in dichloromethane was sandwiched between two sodium chloride crystal cells, which were then placed in the sample holder of the FTIR equipment and scanned through 4000 to 400 cm^{-1}. The X-ray diffraction partners were obtained by use of an X-ray diffractometer (ADX 8000 Mini Ø - Ø).

Investigation of antimicrobial activity of the synthesized AgNPs

A study of the comparative antibacterial activity of the *V amygdalina* extract, ciprofloxacin (positive control), $AgNo_3$ (precursor), and AgNPs was carried out to situate the antimicrobial effectiveness of the AgNPs. A slight modification of the procedure for bacterial broth preparation and plate inoculation reported by Droepenu et al. [24] and cited in Droepenu et al. [26] was used for the investigation using 500 ppm concentration of each preparation. Briefly, a 5.40 ± 0.74 g weight of dried broth was dissolved in 400 ml of deionized water, and the solution was autoclaved at 121 ºC for 15 min. Culture strains of *Staphylococcus aureus* (G +ve), *Escherichia coli* (G –ve), and *Exiguobacterium aquaticum* (G +ve) were inoculated under a shaker at 37 ºC for 16 h. The entire surface of the prepared agar plate was streaked with 1.0 ml of the previously prepared bacterial broth. A 10 µl volume of the Ciprofloxacin, *V amygdalina* leaf extract, $AgNO_3$, and AgNP solutions were each pipetted and dropped onto the surface of the agar disk (6 mm diameter), gently pressed down, and allowed to stand at room temperature for 10 min. The various plates were incubated at 37 ºC for 16 h, and thereafter, the inhibition zones of the preparation were measured in millimeters. Testing was done in triplicate with values expressed as mean ± SD, and data was analyzed by one-way analysis of variance. Significant differences were concluded at p≤0 05 [27].

Results and Discussion

Synthesis of AgNPs

As the solution of the V. amagdalina extract was being added in a dropwise manner into the $AgNO_3$ solution with continuous shaking, the mixture suddenly turned pale yellow from an initial dark greenish color and eventually to dark brown upon standing for 15 min. Figure 1(III) shows the color transition during the synthesis process. Wani [28] noted that biologically synthesized AgNP solutions characteristically exhibit color transition as evidence of the reduction of the $AgNO_3$ to AgNPs. Previous authors have also reported Abrupt color change signaling the formation of AgNPs during biological synthesis [29,30], who attributed it to the formation of surface plasmon resonance (SPR).

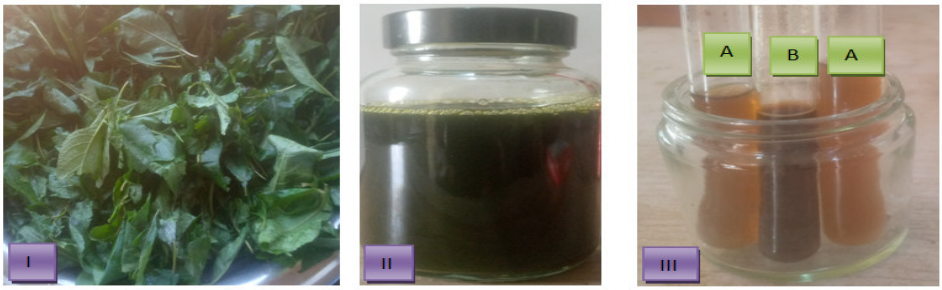

Figure 1 (i-iii). i: Fresh bitterleaves, ii: Crude greenish extract, iiiA: Spontaneously formed yellow coloured AgNP solution and iiiB: AgNP solution turned dark brown upon standing.

Phytochemical analysis of extract

Some of the identified phytoconstituents of the bitterleaf methanol extract are listed in Table 1. The results showed that the extract contained a relatively high proportion of saponins, alkaloids, phenols, and flavonoids but a moderate proportion of tannins and a low content of carbohydrates and terpenoids. Reducing sugar was not detected in the extract. Previous works that used aqueous extract reported a similar trend in the relative abundance of various phytochemicals in *V. amygdalina* extract [16] and concluded that the sticky texture of bitter leaf extract was due to the low content of tannins.

Researchers agree that bioactive phytoconstituents like phenolic compounds, saponins, polysaccharides, flavonoids, and others are responsible for the reducing properties of plant extracts [31]. These phytochemicals facilitate reduction reaction by donating free electrons to some circulating positively charged metal ions, thereby converting the latter to neutral free metal nanoparticles.

Table 1. Phytochemical constituents of *V. amygdalina* extract.

Phytoconstituents	Relative abundance
Saponins	+++
Flavonoids	+++
Terpentoins	++
Phenolic compounds	+++
Tannins	+
Carbohydrates	+
Alkaloids	+++
Reducing sugar	-

Ultraviolet-visible light spectral analysis of AgNPs

Figure 2 shows the UV-vis light spectrum of the AgNP solution. The wavelength of maximum light absorption (λmax) was observed to be 420 nm. This value was within the general range of 400 - 450 nm reported in previous works, which also observed that values above the upper limit are associated with aggregated nanoparticles. In contrast, shifts below the lower limit may be suggestive of the presence of impurities [30]. SEM studies of our synthesized AgNPs revealed predominantly non-aggregated particles. The spectral characteristics of AgNPs are believed to be influenced by the presence of surface plasmon resonance (SPR), a phenomenon attributed to the interaction between incident radiations and oscillating band electrons on the surfaces of the silver nanoparticles [32]. SPR is also thought to arise

from changes in the local dielectric constant at the interface between the nanoparticles and the surrounding medium, including adsorbed phytomolecules [28]. The occurrence of SPR in biogenically synthesized nanoparticles may be suggestive of the presence of adsorbed or conjugated biomolecules on the surfaces of nanoparticles. Many factors such as size, shape, concentration, medium dielectric constant, and the chemical environment of the AgNPs influence the SPR and, invariably, the λmax [33].

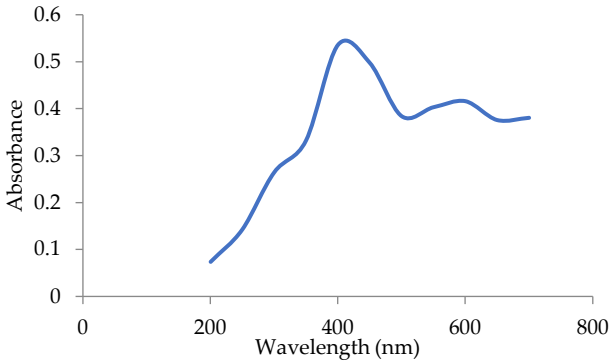

Figure 2. Uv-vis absorbance spectrum of AgNPs solution.

Particle size distribution, polydispersity index and zeta potential of AgNPs

Particle size distribution

The result of the dynamic light scattering (DLS) investigation gave the particle size distribution histogram shown in Figure 3. The mean particle size (Z average) was 74.231 nm. This size was within the nanoscale range of 1 - 100 nm, suggesting that AgNPs were actually synthesized in the current work. The bioactive components of the extract acted as reducing agents that converted Ag+ to free AgNPs. The polydispersity index was 0. 645. This value is an indication that the particles were mono-dispersed. PDI values less than one indicate particle size uniformity [34]. The average zeta potential (ZP) of particles suggests the predominating charge environment/ species close to the surfaces of the particles. The ZP of the synthesized AgNPs was (+) 32.045 mV. This relatively high positive ZP may be responsible for the predominantly non-aggregation of the particle, as observed in the SEM analysis [35]. Similarly, charged particle surfaces tend to experience interparticulate repulsion, thereby preventing aggregation of the various particles [34].

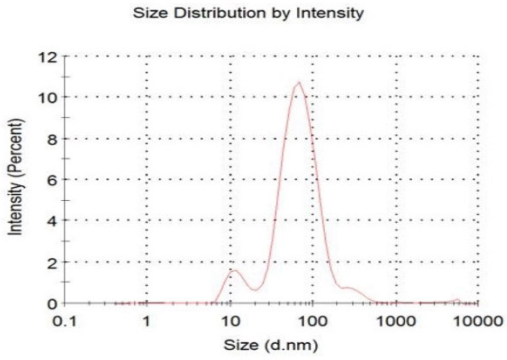

Figure 3. AgNPs particle size distribution curve.

FTIR spectroscopic analysis of the synthesized AgNPs

Figure 4 shows the FTIR spectral readings of the AgNP samples. The components of the spectrum show the presence of peak bands representing functional groups that are not characteristic of pure silver metal. It is known that FTIR spectroscopy cannot read pure atoms or monoatomic ions like Ag or Ag+ alone [36]. Therefore, the presence of the various peaks may have arisen from biomolecules of the *V amygdalina* extract attached to the surfaces of the AgNPs, which caused the bioreduction reactions. Such conjugations enable the biomolecules to play capping and stabilizing roles in the nanoparticle entity. FTIR spectrum can also reveal a compound's molecular composition by identifying characteristic functional group peaks. The observed peaks in functional group assignments are shown in Table 2.

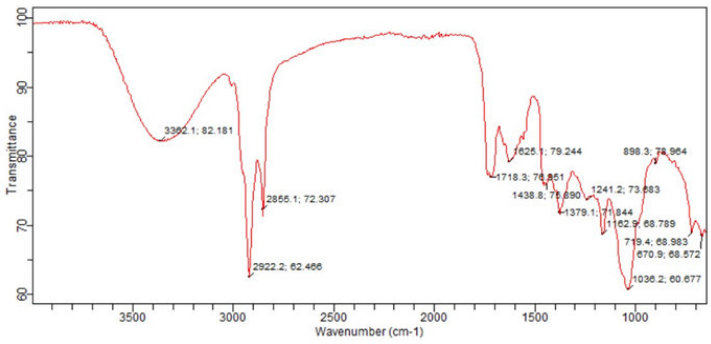

Figure 4. AgNPs FTIR spectrum.

Table 2. FTIR spectral bands and functional group assignment.

Frequency (cm)-1	Spectral peak assignment
3362.1	OH stretching of alcohol and phenols in the extract
2855.1	C∧N stretching
2922.2	C- H stretching
1718.3	C- C stretching
1428..4	N- H stretching in amide linkage
1379.0	N=O symmetry stetching in nitro compounds
719.4	Bonding of metal particles with oxygen

SEM analysis of synthesized AgNPs

Figure 5 (x500) gives the surface morphology of silver nanoparticles synthesized from leaf extract of *V. amygdalina*. It elucidates the individual silver nanoparticles as well as a few aggregates. Rozhin et al. [5] noted that the capping activity of the plant metabolites prevents self-aggregation among the individual nanoparticles. The nanoparticles were predominantly spherical in shape. This was in consonant with earlier works such as Aisida et al. [4], Vanaja et al. [37] and Singh et al. [38] reportedly synthesized spherical-shaped AgNPs through various biogenic processes. Reports by Aisida et al. [4] noted that AgNP shapes are influenced by factors like pH and temperature but not by the concentration of the precursor material. Ye et al. [39] observed that sphericity confers added therapeutic advantages to the nanoparticles since it may enhance their free blood circulation, membrane permeability, and binding affinity. Further, Figure 6 shows the TEM micrograph of the synthesized nanoparticles. The structure suggested the existence of a number of disaggregated crystalline particles.

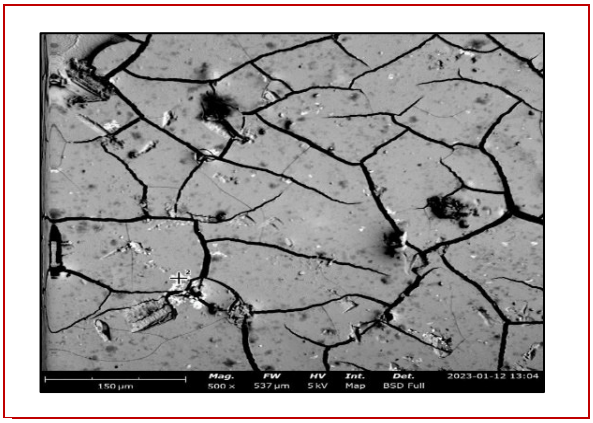

Figure 5. SEM of synthesized silver nanoparticles thin film.

Figure 6. TEM micrograph of AgNPs.

Energy dispersive x–ray (EDX) diffraction analysis

The elemental compositions of the biosynthesized silver nanoparticles are shown in Figures 7 and 8. The reduced silver nanoparticles were subjected to EDX analysis, and signals with an optical absorption characteristic peak at 3 keV were observed. The atomic concentration of the AgNPs was 2.52 %, with a weight concentration of 7.70 %. Vanaja et al. [37] reported that silver nanoparticles showed distinctive absorption peaks at 3 keV. Therefore, this finding is in consonant with earlier works. Other elemental components of the AgNPs with their relative atomic and weight percentages. The tiny multiple peaks of Figure 9 (A and B) signified the high crystallinity of the AgNO3 AgNPs structures. The weak silver peak recorded by EDX (Figure 7 might be due to the low concentration of silver nitrate used in the biosynthesis of the silver nanoparticles. In this work, 100 ml of 1 mM $AgNO_3$ was combined with 10 ml of aqueous leaf extract of *V. amygdalina*, which resulted in a more dilute mixture than that of Vanaja et al. [37] in which 10 ml of freshly prepared stem extract was added into 90 ml of 1 mM silver nitrate solution giving a total reaction volume of 100 ml, and consequently a higher concentration mixture.

It is likely that even though AgNPs were deposited, a relationship exists between the concentration of the $AgNO_3$ used as starting material in the green synthesis and the intensity of the peak of AgNPs produced. Parit et al. and Melita et al. [40, 37] reported that XRD peaks were observed at (111), (200), (220), and (311) when a high concentration of $AgNO_3$ was used but shifted to (122) and (231) when a lower concentration was used for the test.

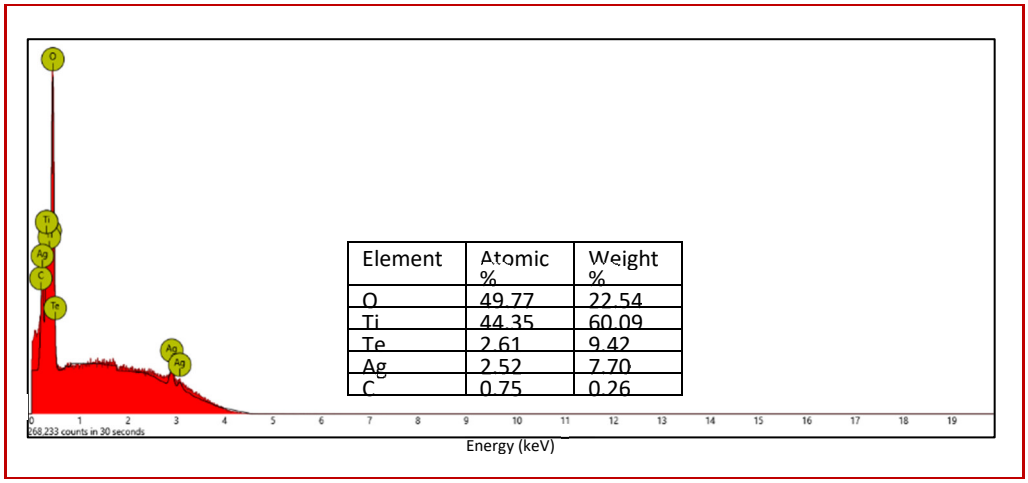

Element	Atomic %	Weight %
O	49.77	22.54
Ti	44.35	60.09
Te	2.61	9.42
Ag	2.52	7.70
C	0.75	0.26

Figure 7. EDX spectrum of AgNPs showing elemental composition.

Microbial activity of the synthesized AgNPs

Table 3 displays the values of the zone of inhibition of the growth of selected microbial species, namely, *Staph aureus, E coli, E aquaticum, and C albican* by the extract, control drugs, the AgNPs, and the precursor $AgNO_3$ solution. It was observed that ciprofloxacin exhibited the largest zones of inhibition against all the three bacterial species but produced no inhibition in the *C albican* isolate. This observation is in tandem with the literature report that ciprofloxacin is a potent antibiotic with broad-spectrum antibacterial activity against many Gram-positive and Gram-negative bacteria but has no intrinsic antifungal effects [41].

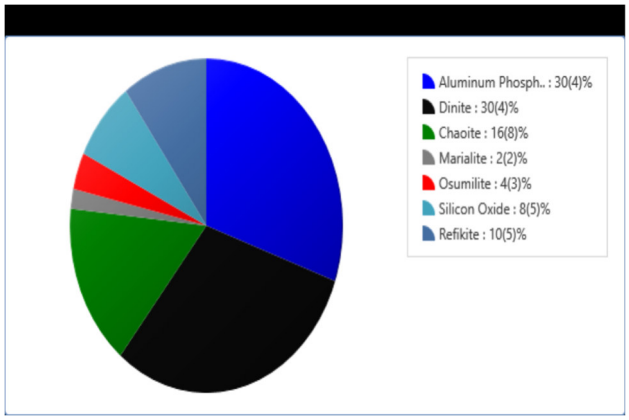

Figure 8. Pie chart representation of EDX spectrum and elemental composition of AgNPs.

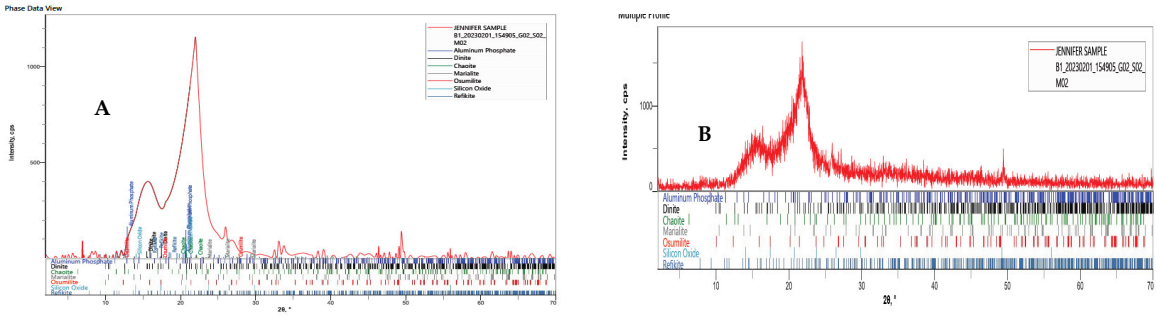

Figure 9 (A & B). EDX spectra showing multiple tiny peaksnity.

On the contrary, Amphotericin B exhibited a relatively large zone of inhibition on the fungal disk but none on the bacterial disks, reflecting the known pharmacological activities of the drug as a weak antibacterial but strong fungicidal agent [42]. The raw *V. amygdalina* extract and the $AgNO_3$ salt

exhibited antibacterial and antifungal effects. Again, the antibacterial and antifungal activity of silver salts and *V. amygdalina* extract has been reported [43]. The results clearly showed that for all the organisms, the AgNPs caused more significant growth inhibition than the raw extract and the precursor $AgNO_3$ salt. The zones of inhibition produced by the AgNPs were comparable to those of the ciprofloxacin. This observation suggested that nanosization enhanced the antimicrobial activity of both the extract and the $AgNO_3$, and this is likely due to the surface conjugation of the *V. amygdalina* biomolecules and the AgNPs, causing either additive or synergistic effects. Tests were carried out in replicates whereby recorded values were equal to mean ± standard deviation (SD), and significant differences were concluded at $p \leq 0.05$ from data analyzed using analysis of variance (ANOVA) statistic and Turkey HSD. Figure 10 shows the zones of inhibition caused by the pure extract, AgNP, as well as Ciprofloxacin and Amphotericin B (positive controls for antibacterial and antifungal agents, respectively).

Table 3. Bacterial and fungal zones of inhibition of various test and control materials.

Material (500 ppm)	Mean zone of inhibition (mm)			
	Organism			
	Staph aureus	*E. coli*	*E. aquaticum*	*C. albican*
Ciprofloxacin	1.97 ± 1.3	1.87 ± 0.5	1.43 ± 1.2	-
Extract	1.02 ± 0.7	1.31 ± 0.3	1.03 ± 0.8	0.85 ± 0.5
$AgNO_3$	1.43 ± 0,5	1.26 ± 2.6	1.21 ± 2.4	0.75 ± 0.3
AgNPs	1.67 ± 0.4	1.54 ± 1.3	1.33 ± 0.7	1.14 ± 0.8
Amphotericin B	-	-	-	1.68 ± 0.3

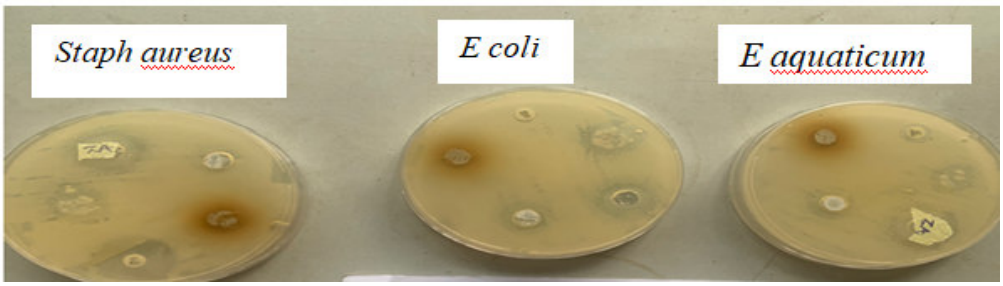

Figure 10. Antimicrobial activities of ciprofloxacin, Amphotericin B, AgNO3, V amygdalina extract and AgNPs against sample bacteria species (see table 3 for dimensions).

Conclusion

Phytochemicals in the *V. amygdalina* extract mediated the conversion (reduction) of $AgNO_3$ molecules to free AgNPs by donating free electrons to neutralize positive charges of circulating silver ions (Ag^+). The synthesized AgNPs exhibited characteristic SPR features and evidence of biomolecule attachment on the surfaces of the nanoparticles, which were predominantly spherical in shape, disaggregated, and had a mean particle size of 74.231 nm. Current findings align with previous researchers who reported low tannin content in the *V. amygdalina* extract. Although the *V Magdalena* extract and the $AgNO_3$ possessed intrinsic anti-pathogenic properties, conjugating them via the AgNP complex enhanced their antibacterial and fungicidal activities. The choice of extracting solvent does not significantly affect the properties of AgNPs produced since the characteristics of the current AgNPs compared well with those reported in the literature, which were synthesized using other extraction solvents.

Acknowledgements

The authors now acknowledge Mallam Isah Yakubu of the Department of Chemical Engineering, Ahmad Bello University Zaria, Nigeria, for his technical support during the spectroscopic analysis of our samples.

Authors contribution

All the authors have contributed equally.

Declaration of interest

The authors declare no conflict of interest.

Financial support

This work has not received any funds from national and international agencies.

References

1. Kumar DA, Kumar V, Palanichamy SM, Roopan SM. Green synthesis of silver nanoparticles using Alternanthera dentata leaf extract at room temperature and their antimicrobial activity. Spectrochimica Acta Part A-Mole. Biomole. Spectros. 2014;127:168-71.
2. Arya G, Kumari RM, Sharma N, Gupta N, Kumar A, Chatterjee S, et al. Catalytic, antibacterial and antibiofilm efficacy of biosynthesized silver nanoparticles using Prosopis juliflora leaf extract along with their wound healing potential. J Photochem Photobiol B. 2019;190:50-8.
3. Yallappa S, Manjanna J, Dhananjaya BL. Phytosynthesis of stable Au, Ag and Au–Ag alloy nanoparticles using J. Sambac leaves extract, and their enhanced antimicrobial activity in presence of organic antimicrobials. Spectrochim. Acta Part A Mol Biomol Spectrosc. 2015;137:236-43.
4. Aisida SO, Ugwu K, Akpa PA, Nwanya AC, Nwankwo U, Botha SS, et al. Biosynthesis of silver nanoparticles using bitter leaf (Vernonia amygdalina) for antibacterial activities. Elsevier: Surfaces and Interfaces. 2019; 17(100359):1-7.
5. Rozhin A, Batasheva S, Kruychkova M, Cherednichenko Y, Rozhina E, Fakhrullin R. Biogenic Silver Nanoparticles: Synthesis and Application as Antibacterial and Antifungal Agents. Micromachines. 2021;12(12): 1480.
6. Jeevanandam J, Barhoum A, Chen SY, Dufresne A, Danquah MK. Review of nanoparticles and nanostructured material toxicity and regulations. Beilstein J Nanotechnol. 2018;9:1050-74.
7. El-Baghdady KZ, El-Shatoury EH, Abdullah OM, Khalil MMH. Biogenic production of silver nanoparticles by Enterobacter cloacae Ism26. Turk J Biol. 2018:42(4): 319-28.
8. Vance ME, Kuiken T, Vejerano EP, McGinnis SP, Hochella Jr MF, Rejeski D, et al. Nanotechnology in the real world: Redeveloping the nanomaterial consumer products inventory. Beilstein J Nanotechnol 2015;6:1769-80.
9. Alshehri AH, Jakubowska M, Młoz˙niak A, Horaczek M, Rudka D, Free C, et al. Enhanced electrical conductivity of silver nanoparticles for high Frequency electronic applications. ACS Appl Mater Interfaces. 2012;4(12): 7007–10.
10. Qidwai A, Pandey A, Kumar R, Shukla SK, Dikshit A. Advances in Biogenic Nanoparticles and the Mechanisms of antimicrobial Effects, Indian J Pharm Sci. 2018;80(4):592-603.
11. Igile GO, Oleszek W, Jurzysta M, Burda S, Fafunso M, Fasanmade AA. Flavonoids from Vernonia amygdalina and their antioxidant activities. J Agric Food Chem. 1994;42(11):2445-8.
12. Oyeyemi IT, Akinlabi AA, Aderiike AG, Aleshinloye A, Oyeyemi OT. Vernonia amygdalina: A folkloric herb with anthelminthic properties: Beni-Suef Univ J Basic Appl Sci. 2018;7(1):43-9.
13. Komlaga G, Agyare C, Dickson RA, Mensah MLK, Annan K, Loiseau PM, et al. Medicinal plants and finished marketed herbal products used in the treatment of malaria in the Ashanti region, Ghana. J Ethnopharmacol. 2015;172:333-46.
14. Agbodeka K, Gbekley HE, Karou SD, Anani K, Agbonon A, Tchacondo T, et al. Ethnobotanical study of medicinal plants used for the treatment of malaria in the Plateau region, Togo. Pharmacognosy Res. 2016;8(Suppl 1):S12-8.
15. Inusa A, Sanusi SB, Linatoc AC, Mainassara MM, Awawu JJ. Phytochemical analysis and antimicrobial activity of bitter leaf (vernonia amygdalina) collected from lapai, niger state, nigeria on some selected pathogenic microorganisms. Scince World Journal. 2018;13(3):15-8.
16. Johnbull OA. Studies on tablet and capsule formulations of vernonia amygdalina dry leaf extract for the management of diabetes [dissertation]: University of Benin, Benincity. Nigeria: 2018.
17. Akah PA, Alemji JA, Salawu OA, Akunne TC, Offiah NV. Effects of Vernonia amygdalina on biochemical and hematological parameters in diabetic rats. Asian J Med Sci. 2009;1(3):108-113.
18. Ugwu CE, Olajide JE, Alumana EO, Ezeanyika LUS. Comparative Effects of the leaves of Vernonia amygdalina and Telfairia occidentalis incorporated diets on the lipid profile of rats. Afri J Biochem Res. 2011;5(1):28-32.

19. Rizwana H, Alwhibi MS, Al-Judaie RA, Aldehaish HA, Alsaggabi NS. Sunlight-Mediated Green Synthesis of Silver Nanoparticles Using the Berries of Ribes rubrum (Red Currants): Characterisation and Evaluation of their Antifungal and Antibacterial Activities. Molecules. 2022;27(7):2186.
20. Sumbal, Nadeem A, Naz S, Ali JS, Mannan A, Zia M. Synthesis, characterization and biological activities of monometallic and bimetallic nanoparticles using Mirabilis jalapa leaf extract. Biotech Rep (Amst). 2019;22:e00338.
21. Patra JK, Baek KH. Green synthesis of silver chloride nanoparticles using Prunus persica L. outer peel extract and investigation of antibacterial, anticandidal, antioxidant potential. Green Chem Lett Rev. 2016;9(2):132-42.
22. Qu J, Yuan X, Wang X, Shao P. Zinc accumulation and synthesis of ZnO nanoparticles using Physalis alkekengi L. Environ Pollut. 2011;159(7):1783-8.
23. Ndikau M, Noah NM, Andala DM, Masika E. Green Synthesis and Characterization of Silver Nanoparticles Using Citrullus lanatus Fruit Rind Extract. Int J Analyti Chem. 2017;2017:8108504.
24. Kwabena DE, Aquisman AE. Morphology of green synthesized ZnO nanoparticles using low temperature hydrothermal technique from aqueous Carica papaya extract. Nanoscience Nanotechnol. 2019;9(1):29-36.
25. Droepenu EK, Asare EA, Wee BS, Wahi RB, Ayertey F, Kyene MO. Biosynthesis, characterization, and antibacterial activity of ZnO nanoaggregates using aqueous extracfrom Anacardium occidentale leaf: comparative study of different precursors. Beni-Suef Univ J Basic Appl Sci. 2021;10(1);1-10.
26. Kwaben DE, Boon SW, Chin S, Kuan YK, Zaini B, Aquisman AE. Comparative evaluation of antibacterial efficacy of biological synthesis of ZnO nanoparticles using fresh leaf extract and fresh stem-bark of Carica papaya. Nano Biomed Eng. 2019;11(3):264-71.
27. Singh Y, Kaushal S, Sodhic RS. Biogenic synthesis of silver nanoparticles using cyanobacterium Leptolyngbya sp. WUC 59 cell-free extract and their effects on bacterial growth and seed germination Nanoscale Adv. 2020; 2:3972-82.
28. Wani IA. Recent advances in biogenic silver nanoparticles and nano composite based plasmonic-colorimetric and electrochemical sensors. ECS J Solid State Sci Technol. 2021;10:047003.
29. Rizwana H, Alwhibi MS, Al-Judaie RA, Aldehaish HA, Alsaggabi NS. Sunlight-Mediated Green Synthesis of Silver Nanoparticles Using the Berries of Ribes rubrum (Red Currants): Characterisation and Evaluation of Their Antifungal and Antibacterial Activities. Molecules. 2022;27(7):2186.
30. Ayad ZM, Ibrahim O, Omar LW. Biosynthesis and characterization of silver nanoparticles by silybum marianum (silymarin) fruit extract. Adv Anim Vet Sci. 2019;7(2):122-30.
31. Dauthal P, Mukhopadhyay M. Noble metal nanoparticles: Plant-mediated synthesis, mechanistic aspects of synthesis, and applications. Ind Eng Chem Res. 2016;55(36):9557-77.
32. Borah SBD, Bora T, Baruah S, Dutta J. Heavy metal ion sensing in water using surface Plasmon resonance of metallic nanostructures. Groundw Sustain Dev. 2015;1(1-2):1-11.
33. He R, Qian X, Yin J, Zhu Z. Preparation of polychrome silver nanoparticles in different solvents. J Mater Chem. 2002;12:3783-6.
34. Sezgin-Bayindir Z, Antep MN, Yuksel N. Development and characterization of mixed niosomes for oral delivery using candesartan cilexetil as a model poorly water-soluble drug. AAPS PharmSciTech. 2014;16(1):108-17.
35. Rai M, Ingle AP, Trzcinska-Wencel J, Wypij M, Bonde S, Yadav A, et al. Biogenic Silver Nanoparticles: WhatWe Know and What Do We Need to Know? Nanomaterials. 2021;11(11):2901.
36. Goel M, Sharma A, Sharma B. Recent Advances in Biogenic Silver Nanoparticles for their biomedical applications. Sustain Chem. 2023;4(1):61-94.
37. Vanaja M, Shanmugan R, Paulkumar K, Gnanajobitha G, Chelladurai M, Gruswamy A. Phytosynthesis and characterization of silver nanoparticles using stem extract of Coleus aromaticus. Int JMater Biomater Applic. 2013;3(1):1-4.
38. Singh P, Kim YJ, Wang C, Mathiyalagan R, Yang DC. The development of a green approach for the biosynthesis of silver and gold nanoparticles by using Panax ginseng root extract, and their biological applications. Artific Cells Nanomed Biotechnol. 2015;44(4):1150-7.
39. Ye H, Shen Z, Yu L, Wei M, Li Y. Manipulating nanoparticle transport within blood flow through external forces: an exemplar of mechanics in nanomedicine. Proc Math Phys Eng Sci. 2018;474(2211):20170845.
40. Parit SB, Karade VC, Patil RB, Pawar NV, Dhavale RP, Tawre M, et al. Bioinspired synthesis of multifunctional silver nanoparticles for enhanced antimicrobial and catalytic applications with tailored SPR properties. Mater. Today Chem. 2020;17:100285.
41. Stergiopoulou T, Meletiadis J, Sein T, Papaioannidou P, Tsiouris I, Roilides E, et al. Isobolographic Analysis of pharmacodynamic interactions between antifungal agents and ciprofloxacin against Candida albicans and Aspergillus fumigates. Antimicrob Agent Chemothera. 2008;52(6):2196-2204.

42. Grela E, Zdybicka-Barabas A, Pawlikowska-Pawlega B, Cytrynska M, Wlodarczyk M, Grudzinski W, et al. Modes of the antibiotic activity of amphotericin B against Candida albicans. Sci Rep. 2019;9:17029.
43. Mehta BK, Chhajlani M, Shrivastava BD. Green synthesis of silver nanoparticles and their characterization by XRD. J Phys Conf Ser. 2017;836:012050.

How to cite this article:
Omeh RC, Ali IJ, Adonu CC. Venonia amygdalina leaf extract - mediated redox synthesis of silver nanoparticles: Characterization and antimicrobial activity. German J Pharm Biomaterials. 2023;2(4):19-30.